Right-handed neutrino dark matter with forbidden annihilation

Yu Cheng,[*] Shao-Feng Ge,[†] Jie Sheng,[‡] and Tsutomu T. Yanagida[§]

Tsung-Dao Lee Institute & School of Physics and Astronomy, Shanghai Jiao Tong University, China and Key Laboratory for Particle Astrophysics and Cosmology (MOE) & Shanghai Key Laboratory for Particle Physics and Cosmology, Shanghai Jiao Tong University, Shanghai 200240, China

(Received 16 April 2023; accepted 21 May 2023; published 12 June 2023)

The seesaw mechanism with three right-handed neutrinos has one as a well-motivated dark matter candidate if stable and the other two can explain baryon asymmetry via the thermal leptogenesis scenario. We explore the possibility of introducing additional particles to make the right-handed neutrino dark matter in thermal equilibrium and freeze out through a forbidden annihilation channel. Nowadays in the Universe, this forbidden channel can be reactivated by a strong gravitational potential such as the supermassive black hole in our galaxy center. The Fermi-LAT gamma ray data and dark matter relic density require this right-handed neutrino dark matter to have mass below 100 GeV and the existence of an additional boson ϕ that can be tested at future lepton colliders.

DOI: 10.1103/PhysRevD.107.123013

I. INTRODUCTION

The heavy right-handed Majorana neutrinos are widely considered as a key ingredient beyond the Standard Model of particle physics. They explain not only the observed tiny neutrino masses via the seesaw mechanism [1–4], but also the Universe's baryon asymmetry through leptogenesis [5]. Normally, we assume three heavy right-handed neutrinos (RHN). However, two heavy Majorana neutrinos are sufficient to explain the observed neutrino oscillation data and the baryon asymmetry in our Universe [6–10]. One remaining right-handed neutrino can be either very heavy or very light [11–15]. In this paper, we explore the latter option that provides us with interesting consequences at low energies.

If the remaining right-handed neutrino is as light as $\mathcal{O}(100)$ GeV, it can be a good candidate of dark matter (DM) [13–18]. However, we have strong constraints from cosmic microwave background (CMB) if they annihilate into the SM particles and the subsequent electromagnetic energy injection affects the ionization history of the Universe [19–29]. Therefore, we consider a forbidden-type DM [30–33] whose freeze-out production is through the annihilation channel to a heavier dark sector partner or SM particles. In other words, DM annihilation is kinematically forbidden. The only way out is the thermal energy that can overcome the mass difference between the initial and final states. This can happen at the early Universe but ceases when the temperature cools down with the Universe expansion. Around the last scattering of CMB photons, the temperature has dropped to eV scale which is negligibly small for any reasonable forbidden DM model. So forbidden DM can avoid those CMB constraints.

Without annihilation at present time, it is very difficult for observation to verify the existence of this forbidden scenario. The indirect detection is intrinsically forbidden. Interestingly, a strong gravitational source, such as a supermassive black hole (SMBH), can reactivate the forbidden DM and make the DM annihilate around it [34]. The subsequent decay of forbidden channel final states into SM particles, especially visible photons, can give a unique indirect detection signature today. The gamma ray from the DM forbidden annihilation only appears in the vicinity around the SMBH, but not anywhere else in the sky. A naive fit with the Fermi-LAT data for Sgr A* shows quite good sensitivity on the thermally averaged annihilation cross section there.

Although the Fermi-LAT constraint is consistent with the DM relic density requirement with naive assignments, a concrete model is necessary to demonstrate the realistic possibility of constructing such a forbidden DM theory. In this paper, we show our right-handed neutrino DM model and its parameter space to generate the correct DM relic density and at the same time provide reactivated

[*]Corresponding author.
chengyu@sjtu.edu.cn
[†]gesf@sjtu.edu.cn
[‡]Corresponding author.
shengjie04@sjtu.edu.cn
[§]tsutomu.yanagida@sjtu.edu.cn

annihilation signal. Comparing with the Fermi-LAT data, we find the right-handed neutrino DM mass is below 100 GeV and the presence of an additional boson ϕ is required in the almost same mass region. Finally, we point out that the possible test at future lepton collider.

II. THE RIGHT-HANDED NEUTRINO FORBIDDEN DM

We assume a Z_2 parity acting only on the right-handed neutrino N to decouple it from all the SM particles. Then, N becomes stable and a good DM candidate [35] (If it is the case, we have an anthropic reason for the presence of three families of quarks and leptons [36].) However, its production is uncertain since it decouples completely from the SM particles. It may be produced in the early Universe through interactions with unknown heavy particles, but its abundance is undetermined by low energy physics.

A possible solution is to introduce a fermion χ and a boson ϕ to couple with the DM N, $\phi N\chi$. Notice here that all fermions, N and χ, are left-handed two component Weyl fermions. The DM neutrino N is assumed to carry odd parity under the Z_2. If ϕ is even (and χ is odd), it can couple to a pair of the SM Higgs bosons, H and $H^\dagger$, via $\phi H^\dagger H$. Thus, the interaction Lagrangian is,

$$\mathcal{L}_{\rm int} = (y\phi N\chi + \text{H.c.}) + \lambda m_\phi \phi H^\dagger H, \tag{1}$$

where m_ϕ is the mass of ϕ. The coupling λ with the SM Higgs boson renders ϕ in thermal equilibrium with the SM particles in the early Universe.

To maintain equilibrium, the decay rate of ϕ to SM fermions, $\Gamma \sim \frac{1}{32\pi}\lambda^2 m_f^2 m_\phi^3/(m_h^2 - m_\phi^2)^2$, should be larger than the Hubble constant $H \propto T_f^2/M_{\rm Pl}$ where $M_{\rm Pl}$ is the Planck mass. Suppose the ϕ decoupling happens around $T_f \sim m_\phi/25$, thermal equilibrium requires $\lambda \gtrsim (10^{-8}$–$10^{-7})$ depending on the scalar mass m_ϕ. Even lower limit is possible if m_ϕ approaches the Higgs mass to reduce the denominator $m_\phi^2 - m_h^2$ of the decay width formula. Further through the Yukawa term and the resulting $NN \leftrightarrow \phi\phi$ scatterings, N can also get in the thermal equilibrium.

All these new particles are singlets of the SM gauge group and have mass terms,

$$\mathcal{L} = \frac{m_N}{2} NN + \frac{m_\chi}{2}\chi\chi + \frac{m_\phi^2}{2}\phi^2. \tag{2}$$

For a forbidden scenario, the DM mass should be lighter than its annihilation final-state particles, $m_N < m_\phi$. Otherwise, the RHN N can pairly annihilate into a pair of ϕ at the late time and then ϕ decays to SM particles through the mixing with the SM Higgs boson. For ϕ mass larger than $\mathcal{O}(1)$ GeV, the dominated decay channel is $\phi \to f\bar{f}$, where $f = b, \tau$. If ϕ mass is $\lesssim \mathcal{O}(1)$ GeV, ϕ can still decay through the diphoton channel $\phi \to \gamma\gamma$ that is induced by triangle diagrams in the similar way as the SM Higgs boson [37]. These processes are strongly constrained by the CMB [38] and high energy gamma ray data [39]. Therefore, we concentrate our discussion on the case that the boson ϕ is heavier than the DM N, $m_\phi > m_N$. Although the DM N may annihilate into SM fermions by exchanging a virtual Higgs, $NN \to \phi + h^*$ and $h^* \to f\bar{f}$, this three-body final state is naturally suppressed by a phase factor $1/16\pi^2 \sim 10^{-2}$ and the Yukawa coupling between Higgs and fermions $y^2 \lesssim 10^{-3}$. In total, it has a $\mathcal{O}(10^{-5})$ suppression relative to the two body annihilation so that the CMB constraint can hardly apply. We also consider that the mass of χ is sufficiently heavy, $m_\chi > m_\phi + m_N$, such that χ can decay and does not contribute to the DM relic density. Below we focus on the density evolution of the right-handed neutrino forbidden DM N.

In the beginning, the DM N is also in thermal equilibrium. It gradually freezes out through the forbidden annihilation channel $N + N \leftrightarrow \phi + \phi$ by exchanging a t-channel χ. The number density evolution is governed by the Boltzmann equation,

$$\dot{n}_N + 3Hn_N = -\langle\sigma_{NN}v\rangle[n_N^2 - (n_N^{\rm eq})^2], \tag{3}$$

where n_N ($n_N^{\rm eq}$) is the number density of right-handed neutrino N (in equilibrium). Since the kinematic threshold of the forbidden channel cuts the allowed range of the center-of-mass energy $\sqrt{s}$, the total cross section cannot easily find an analytical formula. It is more convenient to evaluate the cross section $\langle\sigma_{\phi\phi}v\rangle$ of the reversed process $\phi\phi \to NN$ first and express $\langle\sigma_{NN}v\rangle$ according to detailed balance [30],

$$\langle\sigma_{NN}v\rangle \equiv \left(\frac{n_\phi^{\rm eq}}{n_N^{\rm eq}}\right)^2 \langle\sigma_{\phi\phi}v\rangle = \frac{(1+\delta)^3}{4} e^{-2x\delta}\langle\sigma_{\phi\phi}v\rangle. \tag{4}$$

Being a function of the mass difference $\delta \equiv (m_\phi - m_N)/m_N$ and temperature parameter $x \equiv m_N/T$, the exponential suppression $e^{-2x\delta}$ comes from the ratio of number densities in equilibrium, $n_{\rm eq} = g(mT/2\pi)^{3/2}\exp(-m/T)$, where $g = 2$ and 1 for N and ϕ, respectively. The Boltzmann equation can be solved semianalytically to obtain the rescaled number density $Y_N \equiv n_N/T^3$,

$$Y_N = \frac{[(a - b\delta)\frac{1}{x_f}e^{-2\delta x_f} g_\delta(x_f) + \frac{b}{2x_f^2}e^{-2\delta x_f}]^{-1}}{\sqrt{\frac{\pi}{45}} m_N M_{\rm Pl}(1+\delta)^3 g_*^s/\sqrt{g_*}} \tag{5}$$

where x_f indicates the freeze-out temperature and g_*^s (g_*) the entropy (total) degrees of freedom then. For convenience, we have defined $g_\delta(x_f) \equiv 1 - 2\delta x_f\ e^{2\delta x_f}\int_{2\delta x_f}^\infty t^{-1}\ e^{-t}\ dt$. The parameters a and b are the expansion coefficients of the thermally averaged cross section $\langle\sigma_{\phi\phi}v\rangle$ for the s and p waves, $\langle\sigma_{\phi\phi}v\rangle \equiv a + bx^{-1}$ [40]. The DM relic density is related to Y_N as,

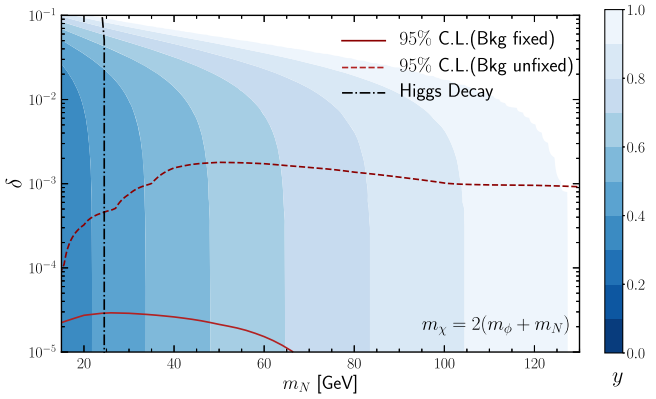

FIG. 1. The allowed parameter space contour to obtain the DM relic density through freeze out. After fixing non-DM fermion mass $m_\chi = 2(m_N + m_\phi)$, there are still three model parameters, the right-handed neutrino DM mass m_N (horizontal axis), the mass difference δ (vertical axis), and the Yukawa coupling constant y (contours according to the color bar). Red lines show the 95% limit provided by the FermiLAT gamma ray data. Both cases with fixed (solid red) and unfixed (dashed red) background are shown for comparison. The almost vertical black dashed line indicates the maximal m_N that allows Higgs invisible decay $h \to N + \chi$.

$$\rho_{\rm DM} = m_N s_0 Y_N, \qquad \Omega_{\rm DM} h^2 = \frac{\rho_{\rm DM}}{\rho_c/h^2}, \tag{6}$$

where $s_0 = 2891.2\ {\rm cm}^{-3}$ is today's entropy density and $\rho_c = 1.05 \times 10^5 h^2\ {\rm GeV/cm}^3$ is the critical density of the Universe.

We also solve the Boltzmann equation numerically with `MicrOMEGAs` [41]. The allowed parameter space to produce the correct relic density $\Omega_{\rm DM} h^2 = 0.12$ is shown in Fig. 1. The two key mass parameters of the forbidden channel are shown in terms of the right-handed neutrino mass m_N and the relative mass difference δ as horizontal and vertical axes, respectively. The whole m_N–δ parameter space is all allowed by tuning the Yukawa coupling y to match the DM relic density. In other words, the value of y is given as a function of m_N, δ, and $\Omega_{\rm DM}$. Although the partner fermion χ also has an adjustable mass m_χ that can enter the annihilation cross section, tuning its value affects the DM relic density in the early Universe and the reactivated forbidden annihilation at current days simultaneously. This resembles the effect of the Yukawa coupling y. Tuning the value of either Yukawa coupling y or m_χ is sufficient for our purpose. For simplicity, we take fixed $m_\chi = 2(m_\phi + m_N)$ for illustration. Figure 1 indicates that the DM relic density naturally limits its mass within the range of $m_N \lesssim 100$ GeV. A smaller coupling constant y prefers smaller DM mass m_N and mass difference δ. This is because when the annihilation cross section becomes smaller, DM freezes out earlier and its number density becomes larger. Since the DM relic density is inversely proportional to the annihilation cross section $\langle \sigma v \rangle$, it scales with m_N^2/y^4. A smaller coupling requires a lighter DM. On the other hand, a smaller mass difference can increase the annihilation cross section to compensate the effect of a small coupling.

III. THE FORBIDDEN DM SIGNATURE

The forbidden DM scenario has an intrinsic difficulty of being probed via indirect detection. Nowadays, the DM Boltzmann distribution with typical $\mathcal{O}(100)$ km/s velocity in our galaxy can no longer support the forbidden channel. Such a nonrelativistic velocity $v \sim 10^{-3}$ can only overcome the mass threshold $\delta \sim v^2 \sim 10^{-6}$. Although direct detection and collider experiments may provide complementary searches and even measure the DM mass, the forbidden nature of DM is still missing. In other words, the theoretical models of forbidden DM can in principle exist but is not testable. This is a very serious issue.

To reopen the forbidden channel, it is necessary to accelerate the DM particles. Around a black hole, especially the SMBH in the galaxy center, a particle can be accelerated to become relativistic because of the strong gravitational force [34]. This can help the DM N to annihilate into heavier dark sector particle ϕ near the SMBH. The unstable ϕ then decays to SM particles through its mixing with the Higgs particle. The decay products are either gamma photons or charged particles. While the di-photon decay channel gives monoenergetic gamma rays in the ϕ rest frame, the charged particles produce photons through final-state radiation or meson decays with continuous spectrum. These allow using gamma ray that can point straightly back to the SMBH as signal for testing our model of right-handed neutrino DM.

The gamma ray intensity highly depends on the DM density and velocity dispersion profiles around the SMBH. In our scenario, DM N has no self-interaction. Thus, its density follows the CDM density profile [42]. For the innermost region, $r < 4GM \equiv r_0$ where M is the BH mass, all particles are attracted to fall into the SMBH so that the DM density is 0 therein. On the other hand, the DM halo simply follows the NFW profile when the gravitational influence of the SMBH no longer dominates which roughly happens at $r_b \equiv 0.2GM/v_0^2$ with v_0 being the DM velocity dispersion there. In between, a DM density spike forms,

$$\rho(r) = \begin{cases} 0, & r < r_0, \ \text{(Capture Region)}, \\ \frac{\rho_{\rm sp}(r)\rho_{\rm in}(t,r)}{\rho_{\rm sp}(r)+\rho_{\rm in}(t,r)}, & r_0 \le r < r_b, \ \text{(Spike)}, \\ \text{NFW Profile}, & r > r_b, \ \text{(Halo)}. \end{cases} \tag{7}$$

Naively thinking, the DM density profiles keeps increasing when going toward the SMBH. However, the DM density

cannot increase forever. In addition to self-interaction, annihilation can also suppresses the growth of DM density. This naturally puts an upper bound on the DM density profile and forms a density plateau around the SMBH. Going inward from the spike region boundary r_b, the DM density profile increases very fast initially as $\rho_{\rm sp}(r) \equiv \rho_b(r_b/r)^{\gamma_{\rm sp}}$ with $\gamma_{\rm sp} \equiv (9-2\gamma_c)/(4-\gamma_c)$. The density coefficient $\rho_b \equiv \rho_D(D/r_b)^{\gamma_c}$ with $\gamma_c = 1$ is scaled according to the NFW profile [43], $\rho(r) \propto 1/r$ for $r \ll 26$ kpc [44,45], from the density around the Solar system with $\rho_D = 0.3$ GeV cm^{-3} and $D = 8.5$ kpc. When reaching the SMBH vicinity, $r \gtrsim r_0$, the DM density increases much slower as $\rho_{\rm in}(r,t) \equiv \rho_{\rm ann}(t)(r/r_{\rm in})^{-\gamma_{\rm in}}$ with $\gamma_{\rm in} = 1/2$. The density $\rho_{\rm ann}$ is the so-called annihilation plateau density $\rho_{\rm ann} \equiv m_N/\langle\sigma_{NN}v\rangle t$. With $\rho = \rho_{\rm sp}\rho_{\rm in}/(\rho_{\rm sp}+\rho_{\rm in})$, its value approaches $\rho_{\rm sp}$ for $\rho_{\rm sp} \ll \rho_{\rm in}$ and $\rho_{\rm in}$ in the opposite. Since $\rho_{\rm sp}(r) \propto r^{-7/3}$ and $\rho_{\rm in}(r) \propto r^{-1/2}$, the DM density profile almost becomes a plateau in the inner spike region. The division $r_{\rm in}$ at $\rho_{\rm sp} = \rho_{\rm ann}$ is determined by the DM annihilation cross section $\langle\sigma_{NN}v\rangle$.

In its vicinity, the SMBH dominates the gravitational potential and consequently the DM velocity dispersion follows a simple scaling $v_d^2(r) \sim GM/r$. In reality, the DM particles inside the spike region are thermalized to a Juttner distribution [46,47] $P_r(V_r, V_c, x(r))$ where V_r is the relative velocity and V_c is the center-of-mass velocity of a two-particle collision system [34]. To get the energy spectrum of the gamma production rate per volume $d\Phi_\gamma(r)/dE_\gamma$, one needs to integrate over the DM distribution from the threshold relative velocity $V_r^{\rm th} \equiv [1-1/(1-2m_F^2/m_\chi^2)^2]^{1/2}$,

$$\frac{dF_\gamma}{dE_\gamma}(r) = \int_{V^{\rm th}}^1 dV_r P_r(V_r, V_c, x(r))\sigma V_r \frac{dN_\gamma}{dE_\gamma}(V_r, V_c), \quad (8)$$

where $x(r)$ has radius dependence through the DM temperature $T = \frac{1}{2}m_N v_d^2(r)$ and dN_γ/dE_γ is the boosted photon spectrum from ϕ decay. For the mass range $m_\phi > 10$ GeV considered in this paper, the dominate channels are $\phi \to b\bar{b}$, $\tau\bar{\tau}$, and gg. We use the PPPC4DMID package [48] to generate the photon spectra of ϕ decay at rest and HDECAY [49] to obtain the branching ratios. After that, we boost the spectrum to the galaxy frame [38,50].

The observed gamma ray flux is an integrated total result over the radius from $r_0 = 4GM$ to some upper limit r_B,

$$\frac{d\Phi_\gamma}{dE_\gamma} = \frac{1}{4\pi D^2}\frac{1}{2m_\chi^2}\int_{4GM}^{r_B} 4\pi r^2 dr \rho^2(r)\frac{dF_\gamma}{dE_\gamma}(r). \quad (9)$$

In principle, the integration upper limit r_B should be as large as possible to include all contributions. However, those DM particles at larger radius have a smaller velocity dispersion and consequently only the tail of the Juttner distribution contributes. To make efficient numerical evaluation, we only include those regions that,

$$\int_{V_r^{\rm th}}^1 dV_r \int_0^1 dV_c P_r(V_r, V_c, x(r_B)) \equiv 1\%. \quad (10)$$

This means that only less than 1% of the DM phase space can contribute at radius larger than r_B.

IV. INDIRECT DETECTION WITH FERMI-LAT

The photon flux from the forbidden annihilation is localized around the SMBH. Uniquely identifying the right-handed neutrino DM scenario requires not just observing the photon spectrum but also good angular resolution. The Fermi-LAT satellite observatory is an all-sky γ-ray telescope with excellent energy and angular resolutions on the γ-ray point source from the GC [51,52]. We analyze a square region of $10° \times 10°$ around Sgr A^* and find several γ-ray point sources, of which 4FGL J1745.6-2859 is the brightest and closest one to Sgr A^* in the Fourth catalog of Fermi-LAT sources (4FGL) [53,54]. This point source is usually considered as the manifestation of Sgr A^* in the MeV-to-GeV range [55]. We use 14 years of Fermi-LAT data from August 4, 2008 to October 26, 2022 in this paper. To be specific, the Pass 8 SOURCE-class events from 100 MeV to 1000 GeV are binned to a pixel size of 0.08°.

A universal model can describe the γ-ray spectrum from point sources. To be specific, this universal 4FGL J1745.6-2859 spectral model is a log-parabola in the 4FGL Catalog [53,54],

$$\frac{dN}{dE} = N_0\left(\frac{E}{E_0}\right)^{-\alpha-\beta\log(E/E_0)}, \quad (11)$$

where N_0 is normalization, E_0 a scale parameter, α the spectral slope at E_0, and β the curvature of the spectrum. Since E_0 does not vary much, its value is fixed to 4074 MeV in our fit while the other three can freely adjust.

For a given DM mass m_N and mass difference δ, the Yukawa coupling constant y is fixed by the DM relic density as explained earlier. This means that the predicted photon flux around the SMBH is also determined for every parameter space point in Fig. 1. We fit the Fermi-LAT data with the following χ^2 function,

$$\chi^2 \equiv \sum_i^{\rm bins}\left(\frac{N_i^{\rm data} - N_i^{\rm bkg} - N_i^{\rm NP}}{\sigma_i}\right)^2. \quad (12)$$

In each bin, $N_i^{\rm data}$ is the data point, $N_i^{\rm bkg}$ the background, $N_i^{\rm NP}$ the expected events due to new physics (NP) contribution, and σ_i the error bar for each data point.

Figure 1 shows the 95% C.L. limit as red lines and the region above are excluded. Since the realistic background is

not determined and the parameters in Eq. (11) are free, we do the fit in two possible ways. We first fix the background to its best-fit values obtained from the background-only hypothesis with $N_0 = 2.519 \times 10^{-12}$, $\alpha = 2.489$, and $\beta = 0.1553$. In this case, the background model can fit data very well and consequently the resulting limit on the signal parameters (red solid line) are quite stringent. The allowed DM mass is below $\lesssim$60 GeV and the mass difference δ cannot be larger than $\mathcal{O}(10^{-5})$. For comparison, we also fit the data by changing both the prediction and background parameters. The corresponding result (red dashed line) allows much larger parameter space with a mass difference as large as 10^{-3}. Both methods require the mass difference within a quite narrow range at the leave of $\mathcal{O}(10^{-5})$ and $\mathcal{O}(10^{-3})$, respectively for DM mass $m_N \gtrsim 30$ GeV.

V. CONCLUSION AND DISCUSSION

In this paper, we propose a model with dark sector including two Majorana fermions N and χ, as well as a Higgs-portal scalar particle ϕ. Among them, the right-handed neutrino N is the lightest one and hence can serve as DM. Its freeze-out production in the early Universe is through the forbidden annihilation channel $N + N \leftrightarrow \phi + \phi$. Although this annihilation channel is nowadays forbidden, it can reopen around a strong gravitation source. Thus, the SMBH located at the galaxy center can accelerate N to make it annihilate into its heavier partner ϕ. The subsequent decay of ϕ to SM particles can bring detectable photon flux. The current Fermi-LAT data requires the right-handed neutrino mass m_N smaller than 100 GeV, and the mass difference $\mathcal{O}(10^{-5}) \lesssim \delta \lesssim \mathcal{O}(10^{-3})$.

Such a light right-handed neutrino can be tested at future lepton colliders such as CEPC [56], ILC [57], FCC-ee [58], and CLIC [59]. If the masses of N and χ satisfy $m_\chi + m_N < m_h$, the SM Higgs particle can decay invisibly, $h \to \chi + N$. For illustration, the projected sensitivity $Br_{\rm inv}^{\rm BSM} < 0.3\%$ at CEPC translates to $\lambda \lesssim 5 \times 10^{-2}$. With our parameter assignments, $m_\phi > m_N$ and $m_\chi > 2(m_N + m_\phi)$, this Higgs invisible decay constraint applies for $m_N < 25$ GeV as shown with vertical black dashed line in Fig. 1. Besides, the dark sector particle ϕ can also be directly produced at future Higgs factories through Higgsstrahlung-like process $e^+ + e^- \to Z + \phi$ [60–66].

In addition to the current model assignments discussed in this paper, there is another possibility of removing the dark sector particle χ and assigning the right-handed neutrino DM N play its role. Then the forbidden annihilation $NN \to \phi\phi$ arises from a much simpler flavor-conserving Yukawa coupling $y\phi NN$. One side effect of this model is introducing DM self-scattering $NN \leftrightarrow NN$ by exchanging a scalar mediator ϕ. Consequently, DM has much a smaller density profile in the spike region. This leads to a weaker constraint on the annihilation cross section [67].

ACKNOWLEDGMENTS

S. F. G. is supported by the Double First Class start-up fund (WF220442604) and National Natural Science Foundation of China (No. 12090064), and Chinese Academy of Sciences Center for Excellence in Particle Physics (CCEPP). T. T. Y. is supported by the China Grant for Talent Scientific Start-Up Project and by Natural Science Foundation of China (NSFC) under grant No. 12175134, JSPS Grant-in-Aid for Scientific Research Grant No. 19H05810, and World Premier International Research Center Initiative (WPI Initiative), MEXT, Japan. Both S. F. G. and T. T. Y. are affiliated members of Kavli IPMU, University of Tokyo.

[1] P. Minkowski, $\mu \to e\gamma$ at a rate of one out of 10^9 muon decays?, Phys. Lett. **67B**, 421 (1977).
[2] T. Yanagida, Horizontal gauge symmetry and masses of neutrinos, Conf. Proc. C **7902131**, 95 (1979).
[3] T. Yanagida, Horizontal symmetry and mass of the top quark, Phys. Rev. D **20**, 2986 (1979).
[4] M. Gell-Mann, P. Ramond, and R. Slansky, Complex spinors and unified theories, Conf. Proc. C **790927**, 315 (1979).
[5] M. Fukugita and T. Yanagida, Baryogenesis without grand unification, Phys. Lett. **174B**, 45 (1986).
[6] P. H. Frampton, S. L. Glashow, and T. Yanagida, Cosmological sign of neutrino *CP* violation, Phys. Lett. B **548**, 119 (2002).
[7] M. Raidal and A. Strumia, Predictions of the most minimal seesaw model, Phys. Lett. B **553**, 72 (2003).
[8] S. L. Glashow, Fact and fancy in neutrino physics. 2., in *10th International Workshop on Neutrino Telescopes* (2003), pp. 611–617, https://inspirehep.net/literature/620998.
[9] V. Barger, D. A. Dicus, H.-J. He, and T.-j. Li, Structure of cosmological *CP* violation via neutrino seesaw, Phys. Lett. B **583**, 173 (2004).
[10] S.-F. Ge, H.-J. He, and F.-R. Yin, Common origin of soft mu-tau and *CP* breaking in neutrino seesaw and the origin of matter, J. Cosmol. Astropart. Phys. 05 (2010) 017.
[11] A. Kusenko, F. Takahashi, and T. T. Yanagida, Dark matter from split seesaw, Phys. Lett. B **693**, 144 (2010).

[12] M. Drewes, The phenomenology of right handed neutrinos, Int. J. Mod. Phys. E **22**, 1330019 (2013).
[13] A. Merle, keV neutrino model building, Int. J. Mod. Phys. D **22**, 1330020 (2013).
[14] M. Drewes *et al.*, A white paper on keV sterile neutrino dark matter, J. Cosmol. Astropart. Phys. 01 (2017) 025.
[15] B. Dasgupta and J. Kopp, Sterile neutrinos, Phys. Rep. **928**, 1 (2021).
[16] A. Kusenko, Sterile neutrinos: The dark side of the light fermions, Phys. Rep. **481**, 1 (2009).
[17] K. N. Abazajian, Sterile neutrinos in cosmology, Phys. Rep. **711–712**, 1 (2017).
[18] A. Boyarsky, M. Drewes, T. Lasserre, S. Mertens, and O. Ruchayskiy, Sterile neutrino dark matter, Prog. Part. Nucl. Phys. **104**, 1 (2019).
[19] R. Bean, A. Melchiorri, and J. Silk, Recombining WMAP: Constraints on ionizing and resonance radiation at recombination, Phys. Rev. D **68**, 083501 (2003).
[20] X.-L. Chen and M. Kamionkowski, Particle decays during the cosmic dark ages, Phys. Rev. D **70**, 043502 (2004).
[21] S. H. Hansen and Z. Haiman, Do we need stars to reionize the universe at high redshifts? Early reionization by decaying heavy sterile neutrinos, Astrophys. J. **600**, 26 (2004).
[22] E. Pierpaoli, Decaying Particles and the Reionization History of the Universe, Phys. Rev. Lett. **92**, 031301 (2004).
[23] N. Padmanabhan and D. P. Finkbeiner, Detecting dark matter annihilation with CMB polarization: Signatures and experimental prospects, Phys. Rev. D **72**, 023508 (2005).
[24] T. R. Slatyer, N. Padmanabhan, and D. P. Finkbeiner, CMB constraints on WIMP annihilation: Energy absorption during the recombination epoch, Phys. Rev. D **80**, 043526 (2009).
[25] L. Roszkowski, E. M. Sessolo, and S. Trojanowski, WIMP dark matter candidates and searches—current status and future prospects, Rep. Prog. Phys. **81**, 066201 (2018).
[26] N. Aghanim *et al.* (Planck Collaboration), Planck 2018 results. I. Overview and the cosmological legacy of Planck, Astron. Astrophys. **641**, A1 (2020).
[27] J. Cang, Y. Gao, and Y.-Z. Ma, Probing dark matter with future CMB measurements, Phys. Rev. D **102**, 103005 (2020).
[28] M. Kawasaki, H. Nakatsuka, K. Nakayama, and T. Sekiguchi, Revisiting CMB constraints on dark matter annihilation, J. Cosmol. Astropart. Phys. 12 (2021) 015.
[29] H. Liu, W. Qin, G. W. Ridgway, and T. R. Slatyer, Exotic energy injection in the early universe II: CMB spectral distortions and constraints on light dark matter, arXiv:2303.07370.
[30] R. T. D'Agnolo and J. T. Ruderman, Light Dark Matter from Forbidden Channels, Phys. Rev. Lett. **115**, 061301 (2015).
[31] A. Delgado, A. Martin, and N. Raj, Forbidden dark matter at the weak scale via the top portal, Phys. Rev. D **95**, 035002 (2017).
[32] R. T. D'Agnolo, D. Liu, J. T. Ruderman, and P.-J. Wang, Forbidden dark matter annihilations into standard model particles, J. High Energy Phys. 06 (2021) 103.
[33] G. N. Wojcik and T. G. Rizzo, Forbidden scalar dark matter and dark Higgses, J. High Energy Phys. 04 (2022) 033.
[34] Y. Cheng, S.-F. Ge, X.-G. He, and J. Sheng, Forbidden dark matter combusted around supermassive black hole, arXiv:2211.05643.
[35] P. Cox, C. Han, and T. T. Yanagida, Right-handed neutrino dark matter in a U(1) extension of the standard model, J. Cosmol. Astropart. Phys. 01 (2018) 029.
[36] M. Ibe, A. Kusenko, and T. T. Yanagida, Why three generations?, Phys. Lett. B **758**, 365 (2016).
[37] R. L. Workman *et al.* (Particle Data Group), Review of particle physics, Prog. Theor. Exp. Phys. **2022**, 083C01 (2022).
[38] G. Elor, N. L. Rodd, T. R. Slatyer, and W. Xue, Model-independent indirect detection constraints on hidden sector dark matter, J. Cosmol. Astropart. Phys. 06 (2016) 024.
[39] G. Fortes, F. Queiroz, C. Siqueira, and A. Viana, Present and future constraints on secluded dark matter in the galactic halo with TeV gamma-ray observatories, arXiv:2212.05075.
[40] P. Gondolo and G. Gelmini, Cosmic abundances of stable particles: Improved analysis, Nucl. Phys. **B360**, 145 (1991).
[41] G. Belanger, A. Mjallal, and A. Pukhov, Recasting direct detection limits within micrOMEGAs and implication for non-standard dark matter scenarios, Eur. Phys. J. C **81**, 239 (2021).
[42] B. D. Fields, S. L. Shapiro, and J. Shelton, Galactic Center Gamma-Ray Excess from Dark Matter Annihilation: Is There A Black Hole Spike?, Phys. Rev. Lett. **113**, 151302 (2014).
[43] J. F. Navarro, C. S. Frenk, and S. D. M. White, The structure of cold dark matter halos, Astrophys. J. **462**, 563 (1996).
[44] G. Alvarez and H.-B. Yu, Density spikes near black holes in self-interacting dark matter halos and indirect detection constraints, Phys. Rev. D **104**, 043013 (2021).
[45] K. N. Abazajian, S. Horiuchi, M. Kaplinghat, R. E. Keeley, and O. Macias, Strong constraints on thermal relic dark matter from Fermi-LAT observations of the Galactic Center, Phys. Rev. D **102**, 043012 (2020).
[46] F. Jüttner, Das Maxwellsche Gesetz der Geschwindigkeitsverteilung in der Relativtheorie, Ann. Phys. (Berlin) **339**, 856 (1911).
[47] S. R. De Groot, *Relativistic Kinetic Theory. Principles and Applications* (1980), ISBN: 9780444854537.
[48] M. Cirelli, G. Corcella, A. Hektor, G. Hutsi, M. Kadastik, P. Panci, M. Raidal, F. Sala, and A. Strumia, PPPC 4 DM ID: A poor particle physicist cookbook for dark matter indirect detection, J. Cosmol. Astropart. Phys. 03 (2011) 051; 10 (2012) E01.
[49] A. Djouadi, J. Kalinowski, and M. Spira, HDECAY: A program for Higgs boson decays in the standard model and its supersymmetric extension, Comput. Phys. Commun. **108**, 56 (1998).
[50] G. Elor, N. L. Rodd, and T. R. Slatyer, Multistep cascade annihilations of dark matter and the Galactic Center excess, Phys. Rev. D **91**, 103531 (2015).
[51] W. B. Atwood *et al.* (Fermi-LAT Collaboration), The large area telescope on the Fermi gamma-ray space telescope mission, Astrophys. J. **697**, 1071 (2009).
[52] A. Albert *et al.* (Fermi-LAT and DES Collaborations), Searching for dark matter annihilation in recently discovered Milky Way satellites with Fermi-LAT, Astrophys. J. **834**, 110 (2017).

[53] S. Abdollahi *et al.* (Fermi-LAT Collaboration), Fermi large area telescope fourth source catalog, Astrophys. J. Suppl. Ser. **247**, 33 (2020).
[54] J. Ballet, T. H. Burnett, S. W. Digel, and B. Lott (Fermi-LAT Collaboration), Fermi large area telescope fourth source catalog data release 2, arXiv:2005.11208.
[55] F. Cafardo and R. Nemmen (Fermi-LAT Collaboration), Fermi-LAT observations of sagittarius A*: Imaging analysis, Astrophys. J. **918**, 30 (2021).
[56] M. Dong *et al.* (CEPC Study Group), CEPC conceptual design report: Volume 2—physics & detector, arXiv:1811.10545.
[57] ILC Collaboration, The International Linear Collider technical design report—volume 2: Physics, arXiv:1306.6352.
[58] A. Abada *et al.* (FCC Collaboration), FCC-ee: The lepton collider: Future circular collider conceptual design report volume 2, Eur. Phys. J. Spec. Top. **228**, 261 (2019).
[59] Physics and detectors at CLIC: CLIC conceptual design report, edited by L. Linssen, A. Miyamoto, M. Stanitzki, and H. Weerts, CERN Yellow Reports: Monographs (CERN, Geneva, 2012), https://inspirehep.net/literature/1090842.
[60] P. Ko and H. Yokoya, Search for Higgs portal DM at the ILC, J. High Energy Phys. 08 (2016) 109.
[61] Z. Heng, W. Wang, and H. Zhou, Higgs-strahlung production of the lightest *CP*-even Higgs boson at ILC in natural NMSSM, Chin. J. Phys. **55**, 1723 (2017).
[62] J. Liu, X.-P. Wang, and F. Yu, A tale of two portals: Testing light, hidden new physics at future e^+e^- colliders, J. High Energy Phys. 06 (2017) 077.
[63] T. Kamon, P. Ko, and J. Li, Characterizing Higgs portal dark matter models at the ILC, Eur. Phys. J. C **77**, 652 (2017).
[64] D. Azevedo, M. Duch, B. Grzadkowski, D. Huang, M. Iglicki, and R. Santos, Testing scalar versus vector dark matter, Phys. Rev. D **99**, 015017 (2019).
[65] B. Grzadkowski, M. Iglicki, K. Mekala, and A. F. Zarnecki, Dark-matter-spin effects at future e^+e^- colliders, J. High Energy Phys. 08 (2020) 052.
[66] G. Haghighat, M. Mohammadi Najafabadi, K. Sakurai, and W. Yin, Probing a light dark sector at future lepton colliders via invisible decays of the SM-like and dark Higgs bosons, Phys. Rev. D **107**, 035033 (2023).
[67] Y. Cheng, S.-F. Ge, J. Sheng, and T. T. Yanagida (to be published).